

# SCIENTIFIC REPORTS



Correction: Publisher Correction

OPEN

## Hydrogen sulfide stimulates CFTR in *Xenopus* oocytes by activation of the cAMP/PKA signalling axis

Alexander Perniss<sup>1,2</sup>, Kathrin Preiss<sup>1</sup>, Marcel Nier<sup>1</sup> & Mike Althaus<sup>1,3</sup>

Hydrogen sulfide (H<sub>2</sub>S) has been recognized as a signalling molecule which affects the activity of ion channels and transporters in epithelial cells. The cystic fibrosis transmembrane conductance regulator (CFTR) is an epithelial anion channel and a key regulator of electrolyte and fluid homeostasis. In this study, we investigated the regulation of CFTR by H<sub>2</sub>S. Human CFTR was heterologously expressed in *Xenopus* oocytes and its activity was electrophysiologically measured by microelectrode recordings. The H<sub>2</sub>S-forming sulphur salt Na<sub>2</sub>S as well as the slow-releasing H<sub>2</sub>S-liberating compound GYY4137 increased transmembrane currents of CFTR-expressing oocytes. Na<sub>2</sub>S had no effect on native, non-injected oocytes. The effect of Na<sub>2</sub>S was blocked by the CFTR inhibitor CFTR\_inh172, the adenylyl cyclase inhibitor MDL 12330A, and the protein kinase A antagonist cAMPS-Rp. Na<sub>2</sub>S potentiated CFTR stimulation by forskolin, but not that by IBMX. Na<sub>2</sub>S enhanced CFTR stimulation by membrane-permeable 8Br-cAMP under inhibition of adenylyl cyclase-mediated cAMP production by MDL 12330A. These data indicate that H<sub>2</sub>S activates CFTR in *Xenopus* oocytes by inhibiting phosphodiesterase activity and subsequent stimulation of CFTR by cAMP-dependent protein kinase A. In epithelia, an increased CFTR activity may correspond to a pro-secretory response to H<sub>2</sub>S which may be endogenously produced by the epithelium or H<sub>2</sub>S-generating microflora.

The cystic fibrosis transmembrane conductance regulator (CFTR) is a chloride and bicarbonate conducting anion channel which is found in many vertebrate epithelia and essential for the epithelial regulation of electrolyte and fluid homeostasis. Gene mutations in CFTR cause cystic fibrosis, the most common autosomal-recessive disorder in Caucasians, with a disease incidence of around 1 in 1000–3000 in northern Europeans<sup>1</sup>. The CFTR protein contains two membrane-spanning regions (each consisting of six transmembrane domains) functioning as the channel pore, which are connected to two intracellular nucleotide binding domains (NBD1 and NBD2) as well as a regulatory (R) domain<sup>2</sup>. NBD1 and NBD2 regulate the opening and closing of the channel by binding and hydrolysing ATP<sup>2,3</sup>, whereas the R-domain initiates the transitions in channel conformation by protein kinase A (PKA)-dependent phosphorylation<sup>2</sup>. Although the NBDs and R-domain contain various phosphorylation sites which control biogenesis, trafficking, interaction with other proteins and channel open probability<sup>2</sup>, PKA is the primary regulator of CFTR activity. At the cellular level, CFTR is hence mainly regulated by cAMP-coupled signalling events.

CFTR is located in the apical membrane of epithelial cells, where it primarily represents a conductance for chloride ions and facilitates transepithelial movement of chloride<sup>4</sup>. CFTR allows chloride permeation in and out of the cells and the direction of chloride flux is determined by the gradient for chloride ions between the cytoplasm and luminal extracellular fluid, as well as the apical membrane potential of the epithelial cells<sup>5</sup>. Whereas CFTR mediates chloride secretion in the intestine, pancreas, secretory coils of sweat glands or serous cells of airway submucosal glands<sup>4,6</sup>, it absorbs chloride in the ducts of sweat glands<sup>4</sup> or, as recently suggested, in the airway surface epithelium<sup>7</sup>. Its physiological importance is also reflected in the consequence of CFTR malfunction and cystic fibrosis phenotype which includes pancreas insufficiency, airway mucus obstruction, meconium ileus and high sweat chloride concentrations<sup>1</sup>. Under physiological conditions, multiple cellular signalling cascades regulate the activity or membrane abundance of CFTR<sup>8</sup>, thus allowing for a precise regulation of chloride flux and, eventually, electrolyte and fluid homeostasis.

<sup>1</sup>Institute for Animal Physiology, Justus-Liebig-University, Giessen, Germany. <sup>2</sup>Present address: Institute for Anatomy and Cell Biology, Justus-Liebig-University, Giessen, Germany. <sup>3</sup>School of Biology, Newcastle University, Newcastle upon Tyne, United Kingdom. Correspondence and requests for materials should be addressed to M.A. (email: [Mike.Althaus@newcastle.ac.uk](mailto:Mike.Althaus@newcastle.ac.uk))

Received: 10 July 2016

Accepted: 5 May 2017

Published online: 14 June 2017

Hydrogen sulfide ( $\text{H}_2\text{S}$ ) is a well-known environmental chemical threat with a characteristic odour of rotten eggs; however, research over the past decade has revealed that  $\text{H}_2\text{S}$  is also an important cellular signalling molecule<sup>9</sup>.  $\text{H}_2\text{S}$  is involved in a variety of physiological and patho-physiological processes (for review see ref.<sup>9</sup>), and  $\text{H}_2\text{S}$ -liberating compounds are currently explored for a therapeutic potential<sup>10</sup>. Physiological concentrations of  $\text{H}_2\text{S}$  are likely in the nano- to low micro-molar range and depend on its production, intracellular storage and mitochondrial degradation<sup>11</sup>.  $\text{H}_2\text{S}$  is enzymatically generated within the metabolism of L-cysteine by cystathionine- $\gamma$ -lyase, cystathionine- $\beta$ -synthase or 3-mercaptopyruvate sulfurtransferase. Enzymatically generated  $\text{H}_2\text{S}$  can either be stored as sulfane sulfur (oxidative formation of protein polysulfides)<sup>12,13</sup>, or degraded by the sulfide oxidation pathway in mitochondria<sup>14</sup>.

In addition to enzymatically generated  $\text{H}_2\text{S}$ , there are exogenous sources of this gas<sup>15</sup>. For example, up to millimolar amounts of  $\text{H}_2\text{S}$  can occur in the digestive tract due to food content and the activity of sulphur-metabolising microbiota<sup>16</sup>. Epithelia are predominantly exposed to exogenous  $\text{H}_2\text{S}$  of environmental or microbiological origin and are challenged to maintain low, physiological  $\text{H}_2\text{S}$  concentrations in order to prevent potential toxicity due to high levels of exogenous  $\text{H}_2\text{S}$ <sup>15,17</sup>. In addition to a high  $\text{H}_2\text{S}$  metabolising capacity in epithelial cells<sup>17</sup>, we recently hypothesised that epithelia use their electrolyte and liquid secreting machinery as a defence strategy in order to flush potentially harmful sources for  $\text{H}_2\text{S}$  from the epithelial surfaces<sup>15</sup>.

In epithelia,  $\text{H}_2\text{S}$  exerts pro-secretory effects by either enhancing the secretion, or decreasing the absorption of electrolytes and liquid across the epithelium<sup>15</sup>. In rat, guinea pig and human colon preparations,  $\text{H}_2\text{S}$  stimulates the secretion of chloride<sup>15</sup>. This is either due to direct actions on ion channels and transporters within the epithelial cells<sup>18,19</sup>, or indirectly by stimulating enteric secretomotor neurons<sup>20</sup>. In rat colon epithelial cells,  $\text{H}_2\text{S}$  induces an increase in the intracellular calcium concentration, which triggers the opening of apical calcium-sensitive chloride channels as well as calcium- and ATP-sensitive potassium channels in the basolateral epithelial cell membrane. This hyperpolarises the apical membrane potential and facilitates apical chloride efflux<sup>18,19</sup>. Similar observations were recently reported in a rat vaginal epithelial preparation, where exogenous  $\text{H}_2\text{S}$  elicits a chloride secretion which involved activation of basolateral ATP-sensitive potassium channels and apical chloride efflux via CFTR<sup>21</sup>. However, the mechanism of how  $\text{H}_2\text{S}$  might facilitate opening of CFTR remains elusive.

In this study we investigated the regulation of CFTR by  $\text{H}_2\text{S}$ . Using heterologous expression of human CFTR in *Xenopus* oocytes, we provide evidence that low-micromolar  $\text{H}_2\text{S}$  concentrations decrease phosphodiesterase activity. This activates the cAMP/PKA signalling axis and triggers activation of CFTR.

## Results

**Hydrogen sulfide stimulates CFTR in *Xenopus* oocytes.** Human CFTR was heterologously expressed in *Xenopus laevis* oocytes and channel activity was measured electrophysiologically by two-electrode voltage-clamp (TEVC) microelectrode recordings. In order to investigate the potential influence of  $\text{H}_2\text{S}$  on heterologously expressed CFTR, the  $\text{H}_2\text{S}$ -forming sulphur salt  $\text{Na}_2\text{S}$  was employed (Fig. 1). The application of  $50\ \mu\text{M}$   $\text{Na}_2\text{S}$  to CFTR-expressing oocytes significantly increased transmembrane currents from  $-0.059 \pm 0.015\ \mu\text{A}$  to  $-0.395 \pm 0.11\ \mu\text{A}$  ( $n = 6$ ;  $N = 3$ ;  $P = 0.0313$ ; Fig. 1a,b). This effect was transient, as transmembrane currents began to decline in the presence of  $\text{Na}_2\text{S}$ . Furthermore, the effect was fully reversible upon removal of  $\text{Na}_2\text{S}$ . In order to confirm expression of CFTR, the cAMP-elevating compounds forskolin ( $5\ \mu\text{M}$ ) and IBMX ( $100\ \mu\text{M}$ ) were applied to the oocyte's superfusate. The application of forskolin/IBMX elicited a significant increase in transmembrane current from  $-0.076 \pm 0.015\ \mu\text{A}$  to  $-1.055 \pm 0.186\ \mu\text{A}$  ( $n = 6$ ;  $N = 3$ ;  $P = 0.0030$ ; Fig. 1a,b). Native oocytes which did not express CFTR did not respond to forskolin/IBMX (Fig. 1c). Transmembrane currents of these oocytes were  $-0.054 \pm 0.026\ \mu\text{A}$  before, and  $-0.056 \pm 0.028\ \mu\text{A}$  after application of the drugs ( $n = 8$ ;  $N = 3$ ;  $P = 0.7525$ ). There was also no effect of  $\text{Na}_2\text{S}$  ( $50\ \mu\text{M}$ ) on native oocytes. Transmembrane currents were  $-0.058 \pm 0.021\ \mu\text{A}$  without and  $-0.057 \pm 0.023\ \mu\text{A}$  with  $\text{Na}_2\text{S}$  ( $n = 8$ ;  $N = 3$ ;  $P = 0.4375$ ; Fig. 1c). However, there was a small but significant increase in transmembrane current from  $-0.027 \pm 0.005\ \mu\text{A}$  to  $-0.035 \pm 0.006\ \mu\text{A}$  when a combination of  $\text{Na}_2\text{S}$  and forskolin/IBMX was applied ( $n = 10$ ;  $N = 2$ ;  $P = 0.008$ ; Fig. 1c).

The  $\text{Na}_2\text{S}$ -induced current of CFTR-expressing oocytes was rapidly inhibited by the additional application of the CFTR inhibitor CFTR\_inh-172 (Fig. 1d,e). Under perfusion with  $50\ \mu\text{M}$   $\text{Na}_2\text{S}$ , transmembrane currents increased to  $-0.757 \pm 0.145\ \mu\text{A}$  and were rapidly inhibited to  $-0.153 \pm 0.039\ \mu\text{A}$  after addition of  $25\ \mu\text{M}$  CFTR\_inh-172 ( $n = 8$ ;  $N = 2$ ;  $P = 0.0078$ ). The transient nature of the current which was stimulated by  $\text{Na}_2\text{S}$  was not the result of a rapid evaporative loss of  $\text{H}_2\text{S}$  from the buffer solutions.  $\text{Na}_2\text{S}$  was measured in the employed buffer solution by the formation of methylene blue and detection of its absorbance at  $670\ \text{nm}$  (Fig. 1f). There was only a minor decrease in methylene blue concentrations over time, indicating that  $\text{H}_2\text{S}$  was present in the buffers even after a time period where current signals began to decline.

In order to confirm that the observed activation of CFTR by  $\text{Na}_2\text{S}$  was due to  $\text{H}_2\text{S}$ , the  $\text{H}_2\text{S}$ -releasing compound GYY4137 which is chemically different from a sulphur salt<sup>22</sup> was employed. Since GYY4137 is a slow-releasing  $\text{H}_2\text{S}$  donor<sup>22</sup>, higher concentrations ( $500\ \mu\text{M}$ ) were used (Fig. 1g,h). GYY4137 elicited a small but significant activation of CFTR. Transmembrane currents of CFTR expressing oocytes significantly increased from  $-0.046 \pm 0.010\ \mu\text{A}$  to  $-0.119 \pm 0.020\ \mu\text{A}$  ( $n = 7$ ;  $N = 2$ ;  $P = 0.0156$ ) due to application of GYY4137 (Fig. 1g,h).

In sum, these data indicate that  $\text{H}_2\text{S}$  activates human CFTR which is heterologously expressed in *Xenopus* oocytes.

**Hydrogen sulfide stimulates CFTR activity via cAMP-mediated signalling events.** The classical intracellular signalling cascade activating CFTR involves adenylyl cyclase (AC)-mediated production of cAMP and subsequent activation of protein kinase A (PKA). PKA phosphorylates the regulatory domain of CFTR and activates the channel in the presence of ATP. In order to investigate whether or not  $\text{H}_2\text{S}$  interferes with this signalling pathway, the effect of the cAMP-elevating drugs forskolin/IBMX was evaluated with or without  $\text{H}_2\text{S}$ .

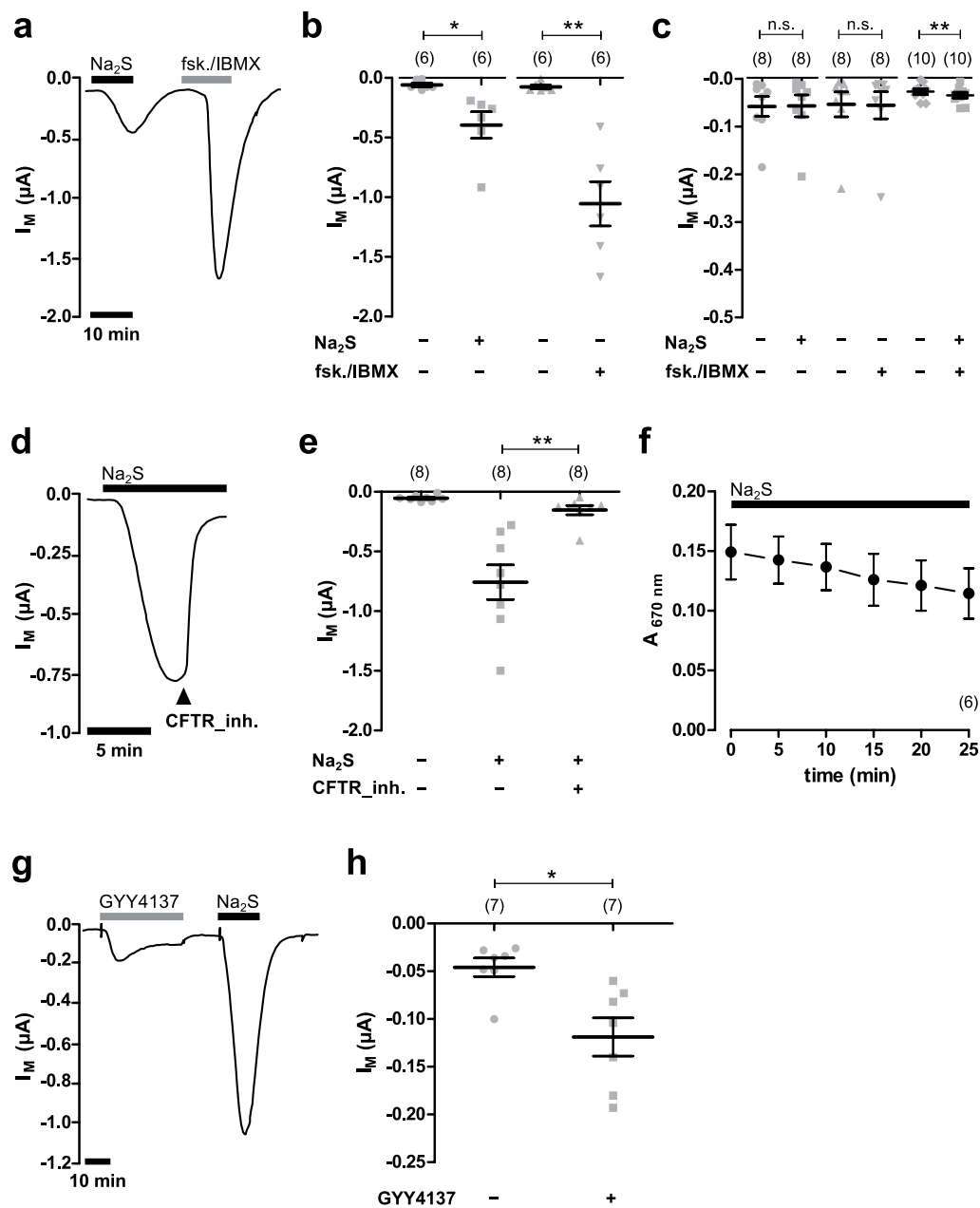


**Figure 1.** Hydrogen sulfide stimulates CFTR in *Xenopus* oocytes. **(a)** A representative current trace of a TEVC recording of a CFTR-expressing oocyte. The application of  $\text{Na}_2\text{S}$  (50 μM, black bar) as well as forskolin (fsk; 5 μM) and IBMX (100 μM; grey bars) led to an increase in transmembrane current signals ( $I_M$ ). **(b)** Statistical analysis of data obtained from experiments as shown in panel a. Depicted are values of  $I_M$  (before drug application or peak values after drug application) from individual experiments (grey symbols) as well as means ± SEM (\* $P \leq 0.05$ , Wilcoxon signed rank test; \*\* $P \leq 0.01$ , Student's paired t-test). **(c)** Summarised data from experiments as similar to those shown in panels a and b, using native, non-CFTR-expressing oocytes. Values of  $I_M$  were taken at time point were CFTR-expressing oocytes of the same donor had the maximal response to the drugs. Depicted are means ± SEM (\*\* $P \leq 0.01$ , Student's paired t-test). **(d)** A representative current trace of a TEVC recording of a CFTR-expressing oocyte. After application of  $\text{Na}_2\text{S}$  (50 μM, black bar), the CFTR inhibitor CFTR\_inh172 (CFTR\_inh.; 25 μM) was additionally applied. This readily inhibited values of  $I_M$ . **(e)** Statistical analysis of data obtained from experiments as shown in panel d. Depicted are values of  $I_M$  (before drug application or peak values after drug application) from individual experiments (grey symbols) as well as means ± SEM (\*\* $P \leq 0.01$ , Wilcoxon signed rank test). **(f)** Evaporative loss of  $\text{H}_2\text{S}$  was measured by monitoring the concentration of  $\text{H}_2\text{S}$  in the employed buffers solutions by the formation of methylene blue. Depicted are values for methylene blue absorbance at 670 nm over time.  $\text{Na}_2\text{S}$  (50 μM) exposure is indicated by the black bar. **(g)** A representative current trace of a TEVC recording of a CFTR-expressing oocyte. Both, GYY4137 (500 μM, grey bar) as well as  $\text{Na}_2\text{S}$  (50 μM, black bar) stimulated  $I_M$ . **(h)** Statistical analysis of data obtained from experiments as shown in panel g. Depicted are values of  $I_M$  (peak values after drug application) from individual experiments (grey symbols) as well as means ± SEM (\* $P \leq 0.05$ , Wilcoxon signed rank test). Numbers of experiments (n) are indicated in parentheses.

The application of forskolin/IBMX elicited a significant and transient increase in transmembrane current (Fig. 2a) from  $-0.064 \pm 0.009 \mu\text{A}$  to  $-1.364 \pm 0.284 \mu\text{A}$  ( $n = 11$ ;  $N = 5$ ;  $P = 0.0009$ ). This effect was fully reversible upon removal of the drugs. A second application of forskolin/IBMX again stimulated CFTR activity from  $-0.081 \pm 0.022 \mu\text{A}$  to  $-0.604 \pm 0.114 \mu\text{A}$  ( $n = 11$ ;  $N = 5$ ;  $P = 0.0038$ ; Fig. 2a). The second effect of forskolin/IBMX was normalised to the effect of the first forskolin/IBMX application and defined as ‘normalised CFTR activity’. Without any additional treatment, control oocytes had thus a normalised CFTR activity of  $0.42 \pm 0.04$  ( $n = 11$ ;  $N = 5$ ). We then applied increasing concentrations of  $\text{Na}_2\text{S}$  after the first application of forskolin/IBMX (Fig. 2a). Interestingly,  $50 \mu\text{M}$   $\text{Na}_2\text{S}$  which elicited robust currents in previous experiments (Fig. 1) did not significantly stimulate transmembrane currents after the oocytes had been exposed to forskolin/IBMX (Fig. 2a,c). Only a high dose of  $300 \mu\text{M}$   $\text{Na}_2\text{S}$  triggered a small increase in transmembrane currents from  $-0.033 \pm 0.010 \mu\text{A}$  to  $-0.051 \pm 0.009 \mu\text{A}$  ( $n = 8$ ;  $N = 3$ ;  $P = 0.0423$ ; Fig. 2a,c). However, despite the lack of an effect of  $\text{Na}_2\text{S}$  after previous exposure of the oocytes to forskolin/IBMX,  $\text{Na}_2\text{S}$  enhanced the second effect of forskolin/IBMX. Normalised CFTR activity dose-dependently increased due to application of  $\text{Na}_2\text{S}$  (Fig. 2a,d). This effect was inhibited by  $25 \mu\text{M}$  of CFTR<sub>inh.172</sub> (Fig. 2b,d). Furthermore, there was only a minor current activation due to  $50 \mu\text{M}$   $\text{Na}_2\text{S}$  and forskolin/IBMX in native, non-CFTR expressing oocytes (Fig. 1c). These data suggest that  $\text{Na}_2\text{S}$  potentiates CFTR-activity which was elicited by forskolin/IBMX.

To investigate if the  $\text{Na}_2\text{S}$ -induced stimulation of CFTR involves AC and PKA, specific inhibitors of these enzymes were employed and  $\text{Na}_2\text{S}$ -induced currents ( $I_{\text{Na}_2\text{S}}$ ) were estimated with or without these drugs (Fig. 3).  $\text{Na}_2\text{S}$  ( $50 \mu\text{M}$ ) was applied twice to CFTR-expressing oocyte in order to control for a potential desensitisation in response to repetitive  $\text{Na}_2\text{S}$ -exposure (Fig. 3a,b). The first  $I_{\text{Na}_2\text{S}}$  was  $0.321 \pm 0.108 \mu\text{A}$  and not significantly different from the second  $I_{\text{Na}_2\text{S}}$  which was  $0.312 \pm 0.087 \mu\text{A}$  (Fig. 3b;  $n = 6$ ;  $N = 5$ ;  $P = 0.854$ ).

MDL 12330 A was used as an inhibitor of AC. In control experiments,  $\text{Na}_2\text{S}$  ( $50 \mu\text{M}$ ) was applied to CFTR-expressing oocytes, which led to an  $I_{\text{Na}_2\text{S}}$  of  $0.130 \pm 0.040 \mu\text{A}$  ( $n = 6$ ;  $N = 2$ ). Afterwards, the oocytes were perfused with DMSO (0.1%; the solvent for MDL 12330A) and stimulated again with  $50 \mu\text{M}$   $\text{Na}_2\text{S}$ . This resulted in an  $I_{\text{Na}_2\text{S}}$  of  $0.085 \pm 0.019 \mu\text{A}$  ( $n = 6$ ;  $N = 2$ ), which was not significantly different ( $P = 0.1395$ ) from the first  $I_{\text{Na}_2\text{S}}$  (Fig. 3c,d). By contrast, when MDL 12330A was applied,  $I_{\text{Na}_2\text{S}}$  significantly decreased from  $0.133 \pm 0.035 \mu\text{A}$  to  $0.011 \pm 0.003 \mu\text{A}$  ( $n = 8$ ;  $N = 2$ ;  $P = 0.0056$ ; Fig. 3c,d).

A similar experiment was performed with cAMPS-Rp – a PKA antagonist – which was directly injected into the oocytes during experiments. For control experiments, CFTR-expressing oocytes were stimulated with  $\text{Na}_2\text{S}$  ( $50 \mu\text{M}$ ). Subsequently,  $9.2 \text{ nl}$  of an intracellular-analogous solution (IAS) was injected into the oocytes and the cells were stimulated a second time with  $\text{Na}_2\text{S}$ . This manoeuvre increased (although values did not reach statistical significance)  $I_{\text{Na}_2\text{S}}$  from  $0.255 \pm 0.046 \mu\text{A}$  to  $0.484 \pm 0.126 \mu\text{A}$  ( $n = 9$ ;  $N = 2$ ;  $P = 0.0743$ ; Fig. 3e,f). A similar observation has been reported in a previous study<sup>23</sup>, where a volume-increase in oocytes increased the activation of CFTR by cAMP-elevating compounds. By contrast, injection of the PKA antagonist cAMPS-Rp abrogated the second effect of  $\text{Na}_2\text{S}$ . Values of  $I_{\text{Na}_2\text{S}}$  significantly decreased from  $0.248 \pm 0.061 \mu\text{A}$  to  $0.011 \pm 0.006 \mu\text{A}$  ( $n = 9$ ;  $N = 2$ ;  $P = 0.0039$ ; Fig. 3e,f). Taken together, these data show that  $\text{H}_2\text{S}$  activates CFTR by cAMP- and PKA-mediated signalling in *Xenopus* oocytes.

**Hydrogen sulfide targets phosphodiesterase rather than adenylyl cyclase.** An increase in intracellular cAMP concentrations could either be the result of enhanced cAMP production by AC, or inhibition of cAMP degradation by phosphodiesterase (PDE).  $\text{H}_2\text{S}$  might thus stimulate AC or inhibit PDE – both effects would result in accumulation of cAMP, a downstream activation of PKA and subsequent stimulation of CFTR. In order to discriminate between AC- and PDE-mediated contributions to CFTR activation, CFTR was stimulated with maximal effective concentrations of either forskolin (AC activator) or IBMX (PDE inhibitor). If  $\text{H}_2\text{S}$  potentiated the effect of forskolin, but not that of IBMX,  $\text{H}_2\text{S}$  likely prevents cAMP degradation by PDE. If  $\text{H}_2\text{S}$  potentiated the effect of IBMX, but not that of forskolin,  $\text{H}_2\text{S}$  likely stimulates cAMP production by AC.

First, we investigated if  $\text{H}_2\text{S}$  affects the effect of forskolin alone (Fig. 4a). Since we were not able to additionally stimulate CFTR activity by increasing the forskolin concentration to  $30 \mu\text{M}$  (data not shown), we considered the employed concentration of  $5 \mu\text{M}$  as maximally effective, an observation which is consistent with a reported  $\text{EC}_{50}$  value of  $\sim 0.07 \mu\text{M}$  for forskolin in airway epithelia<sup>24</sup>. In control experiments, forskolin ( $5 \mu\text{M}$ ) was applied to CFTR-expressing oocytes, which stimulated  $I_{\text{M}}$  by  $0.324 \pm 0.056 \mu\text{A}$  ( $n = 13$ ;  $N = 3$ ). After wash-out, the oocytes were stimulated again with  $5 \mu\text{M}$  forskolin. This resulted in a second stimulation of  $I_{\text{M}}$  by  $0.363 \pm 0.068 \mu\text{A}$  ( $n = 13$ ;  $N = 3$ ; Fig. 4a). The second effect of forskolin was normalised to the effect of the first forskolin application and defined as ‘normalised forskolin effect’ (Fig. 4b). Under these control conditions, the normalised forskolin effect was  $1.135 \pm 0.146$  ( $n = 13$ ;  $N = 2$ ). By contrast, oocytes which were treated with  $50 \mu\text{M}$   $\text{Na}_2\text{S}$  (together with the second application of forskolin) had a significantly enhanced normalised forskolin effect of  $3.054 \pm 0.405$  ( $n = 13$ ;  $N = 3$ ,  $P < 0.0001$ , Gaussian approximation; Fig. 4a,b).

An identical protocol was employed with a high concentration of the PDE inhibitor IBMX ( $1 \text{ mM}$ ) and a ‘normalised IBMX effect’ was estimated (Fig. 4c,d). The normalised IBMX effect was  $0.714 \pm 0.080$  ( $n = 10$ ;  $N = 3$ ) under control conditions, and not significantly different from that which was estimated in the presence of  $\text{Na}_2\text{S}$  which was  $0.966 \pm 0.178$  ( $n = 10$ ;  $N = 3$ ;  $P = 0.2208$ ).  $\text{Na}_2\text{S}$  thus enhanced the effect of the AC-agonist forskolin, but not that of the PDE-inhibitor IBMX.  $\text{H}_2\text{S}$  might therefore impair PDE-mediated cAMP degradation rather than AC-mediated cAMP production.

In order to confirm these observations a different strategy was employed (Fig. 4e-g). AC-mediated cAMP-production was blocked by application of the AC inhibitor MDL 12330 A ( $20 \mu\text{M}$ ) to CFTR-expressing oocytes. Subsequently,  $100 \mu\text{M}$  of membrane-permeable 8-Br-cAMP was applied. This stimulated an increase in transmembrane current ( $I_{\text{cAMP}}$ ) of  $0.056 \pm 0.0221 \mu\text{A}$  ( $n = 7$ ;  $N = 4$ ). After washout of all drugs, MDL 12330 A ( $20 \mu\text{M}$ ) was applied again and  $50 \mu\text{M}$   $\text{Na}_2\text{S}$  was added. Afterwards, 8Br-cAMP was additionally applied and  $I_{\text{cAMP}}$  significantly increased to  $0.590 \pm 0.154 \mu\text{A}$  ( $n = 7$ ;  $N = 4$ ;  $P = 0.0124$ ; Fig. 4e,g). By contrast, there was no

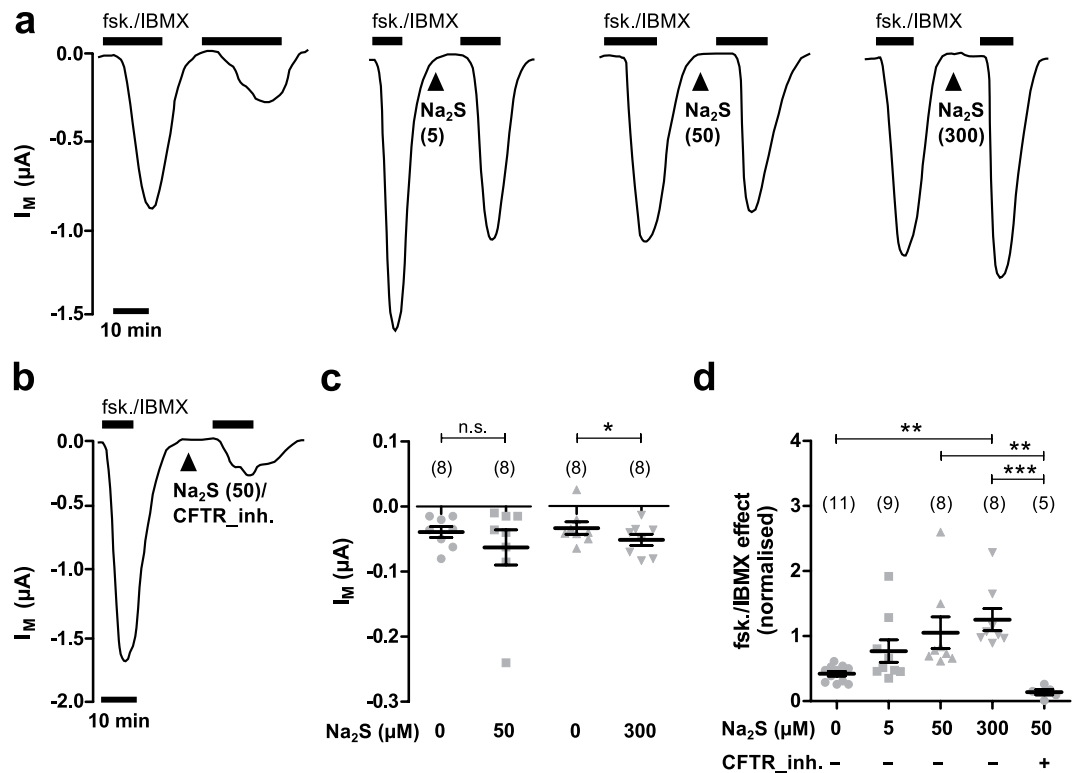


**Figure 2.** H<sub>2</sub>S potentiates the effect of forskolin and IBMX. (a) Representative current traces of TEVC recordings of CFTR-expressing oocytes. Transmembrane currents ( $I_M$ ) were recorded and oocytes were exposed twice to forskolin (fsk., 5  $\mu$ M) and IBMX (100  $\mu$ M, black bars) without or with application of  $\text{Na}_2\text{S}$  (arrowheads; concentration in  $\mu$ M is indicated by numbers in parentheses) between the first and second stimulation with forskolin/IBMX. (b) Representative current trace of a TEVC recording of a CFTR-expressing oocyte. Similar to experiments shown in panel a, oocytes were stimulated twice with forskolin/IBMX and  $\text{Na}_2\text{S}$  (50  $\mu$ M) together with the CFTR inhibitor CFTR\_inh172 (CFTR\_inh., 25  $\mu$ M) between the first and second application of forskolin/IBMX. (c) Statistical analysis of data obtained from experiments as shown in panel a. Depicted are values of  $I_M$  (peak values after drug application) from individual experiments (grey symbols) as well as means  $\pm$  SEM, before and after application of  $\text{Na}_2\text{S}$  (\* $P \leq 0.05$ , Student's paired t-test). (d) Statistical analysis of data obtained from experiments as shown in panels a and b. Depicted are normalised values from individual experiments (grey symbols) as well as means  $\pm$  SEM of forskolin (fsk.)/IBMX effects. This represents the ratio of the first and second current stimulated by forskolin/IBMX (\*\* $P \leq 0.01$ , \*\*\* $P \leq 0.001$ , Kruskal-Wallis test followed by Dunn's Multiple Comparison Test). Numbers of experiments (n) are indicated in parentheses.

difference between the first and second  $I_{\text{cAMP}}$  ( $0.091 \pm 0.026 \mu\text{A}$  and  $0.064 \pm 0.016 \mu\text{A}$ ;  $n = 5$ ;  $N = 2$ ;  $P = 0.1561$ ) when the procedure was repeated without  $\text{Na}_2\text{S}$  (Fig. 4f,g). These data indicate that H<sub>2</sub>S enhances the efficacy of 8-Br-cAMP.

In sum, these data provide evidence that H<sub>2</sub>S inhibits endogenous PDE in *Xenopus* oocytes. This results in cAMP-mediated stimulation of CFTR-activity via downstream activation by PKA.

## Discussion

In this study we investigated the regulation of CFTR by H<sub>2</sub>S. Previous studies using the mouse hippocampal cell line HT22<sup>25</sup> or rat vaginal epithelial preparations<sup>21</sup> suggested that CFTR might be a target for H<sub>2</sub>S. In order to elaborate on this hypothesis, human CFTR was heterologously expressed in *Xenopus* oocytes and functional CFTR expression was confirmed by application of the cAMP-elevating compounds forskolin and IBMX, which resulted in a transient increase in transmembrane currents which did not occur in native, non-injected oocytes. These observations are consistent with previously published functional electrophysiological analyses of human CFTR in *Xenopus* oocytes<sup>23,26</sup>. The H<sub>2</sub>S-liberating sulphur salt  $\text{Na}_2\text{S}$  elicited a transient current stimulation of CFTR-expressing oocytes which was readily inhibited by the CFTR inhibitor CFTR\_inh172 and did not occur in native oocytes. Furthermore, the slow-releasing H<sub>2</sub>S-liberating molecule GYY4137 also stimulated transmembrane currents in *Xenopus* oocytes. These data indicate that H<sub>2</sub>S, released from  $\text{Na}_2\text{S}$  or GYY4137, stimulates CFTR activity.

We then elaborated on the signalling mechanisms which mediate the H<sub>2</sub>S-induced activation of CFTR. We first stimulated CFTR-expressing oocytes with forskolin/IBMX and after removal of these drugs, cells were exposed to H<sub>2</sub>S. Interestingly, a direct response to H<sub>2</sub>S only occurred when high concentrations of  $\text{Na}_2\text{S}$  were employed. When forskolin/IBMX were applied twice to CFTR-expressing oocytes, the second activation by forskolin/IBMX was ~60%



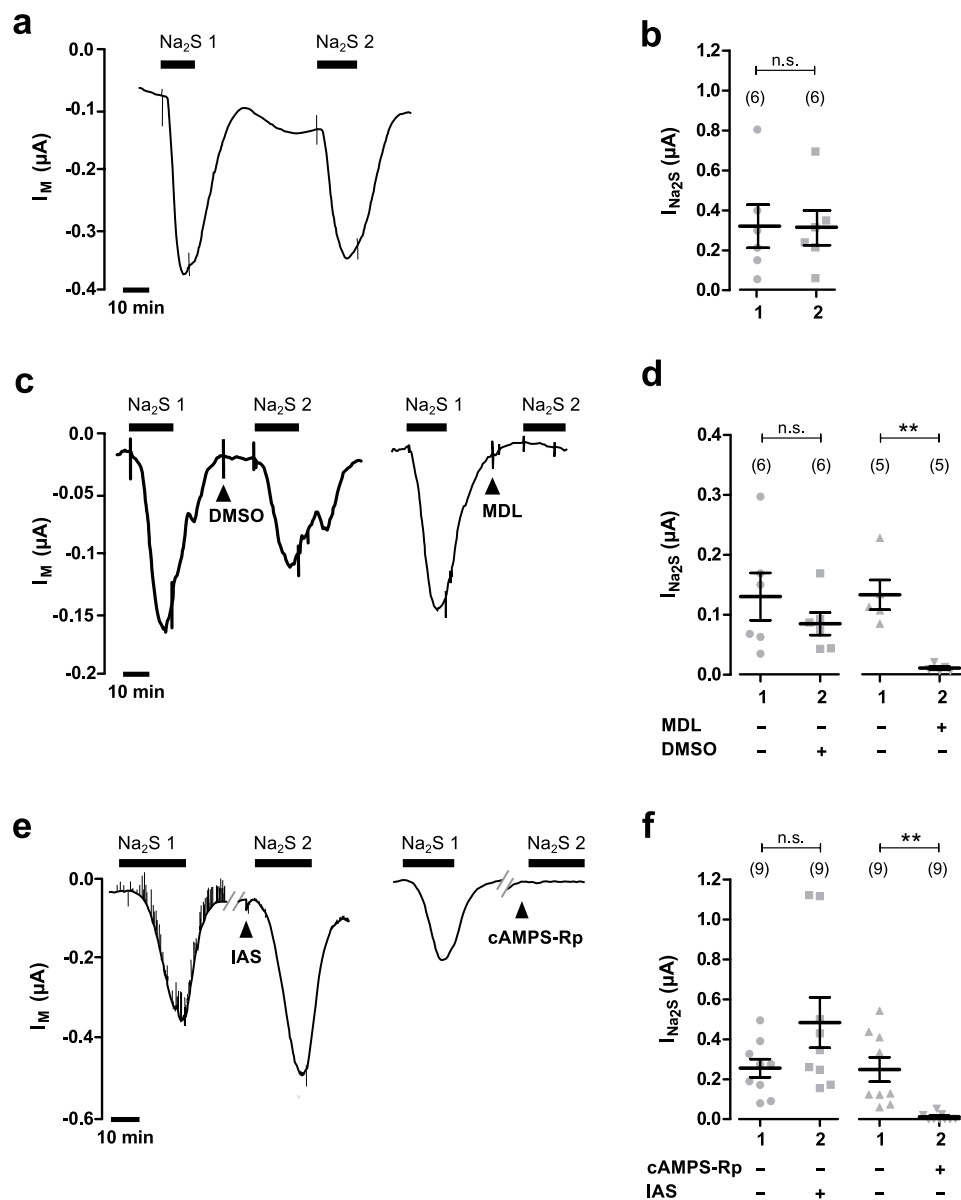


**Figure 3.** H<sub>2</sub>S stimulates CFTR via cAMP- and PKA-mediated signalling. (a) Representative current trace of a TEVC recordings of a CFTR-expressing oocyte. Transmembrane currents ( $I_M$ ) were recorded and the oocyte was exposed twice to Na<sub>2</sub>S (50  $\mu$ M, black bar). (b) Statistical analysis of data obtained from experiments as shown in panel a. Depicted are values of the first (1) and second (2) Na<sub>2</sub>S-induced current ( $I_{Na_2S}$ ) from individual experiments (grey symbols) as well as means  $\pm$  SEM (n.s. = not significant, Student's paired t-test).  $I_{Na_2S}$  was calculated by subtracting the current before application of Na<sub>2</sub>S from the peak value after application of Na<sub>2</sub>S, resulting in positive values for  $I_{Na_2S}$ . (c) Representative current traces of TEVC recordings of CFTR-expressing oocytes. Transmembrane currents ( $I_M$ ) were recorded and oocytes were exposed twice to Na<sub>2</sub>S (50  $\mu$ M, black bar) DMSO (0.1%; left trace) or the AC inhibitor MDL 12330 A (MDL, 20  $\mu$ M; right trace) were applied between the first and second stimulation with Na<sub>2</sub>S (black arrowheads). (d) Statistical analysis of data obtained from experiments as shown in panel a. Depicted are values of the first (1) and second (2) Na<sub>2</sub>S-induced current ( $I_{Na_2S}$ ) from individual experiments (grey symbols) as well as means  $\pm$  SEM (\*\* $P \leq 0.01$ , Student's paired t-test).  $I_{Na_2S}$  was calculated by subtracting the current before application of Na<sub>2</sub>S from the peak value after application of Na<sub>2</sub>S, resulting in positive values for  $I_{Na_2S}$ . (e) Representative current traces of TEVC recordings of CFTR-expressing oocytes. Transmembrane currents ( $I_M$ ) were recorded and oocytes were exposed twice to Na<sub>2</sub>S (50  $\mu$ M, black bar). The perfusion recording was stopped briefly between the first and second stimulation with Na<sub>2</sub>S (grey lines). Then, an intracellular-analogous solution (IAS) or IAS containing the PK-antagonist cAMPS-Rp (87  $\mu$ M) were injected into the oocytes before the second stimulation with Na<sub>2</sub>S (black arrowheads). (f) Statistical analysis of data obtained from experiments as shown in panel a. Depicted are values of the first (1) and second (2) Na<sub>2</sub>S-induced current ( $I_{Na_2S}$ ) from individual experiments (grey symbols) as well as means  $\pm$  SEM (\*\* $P \leq 0.01$ , Wilcoxon signed rank test). Numbers of experiments (n) are indicated in parentheses.

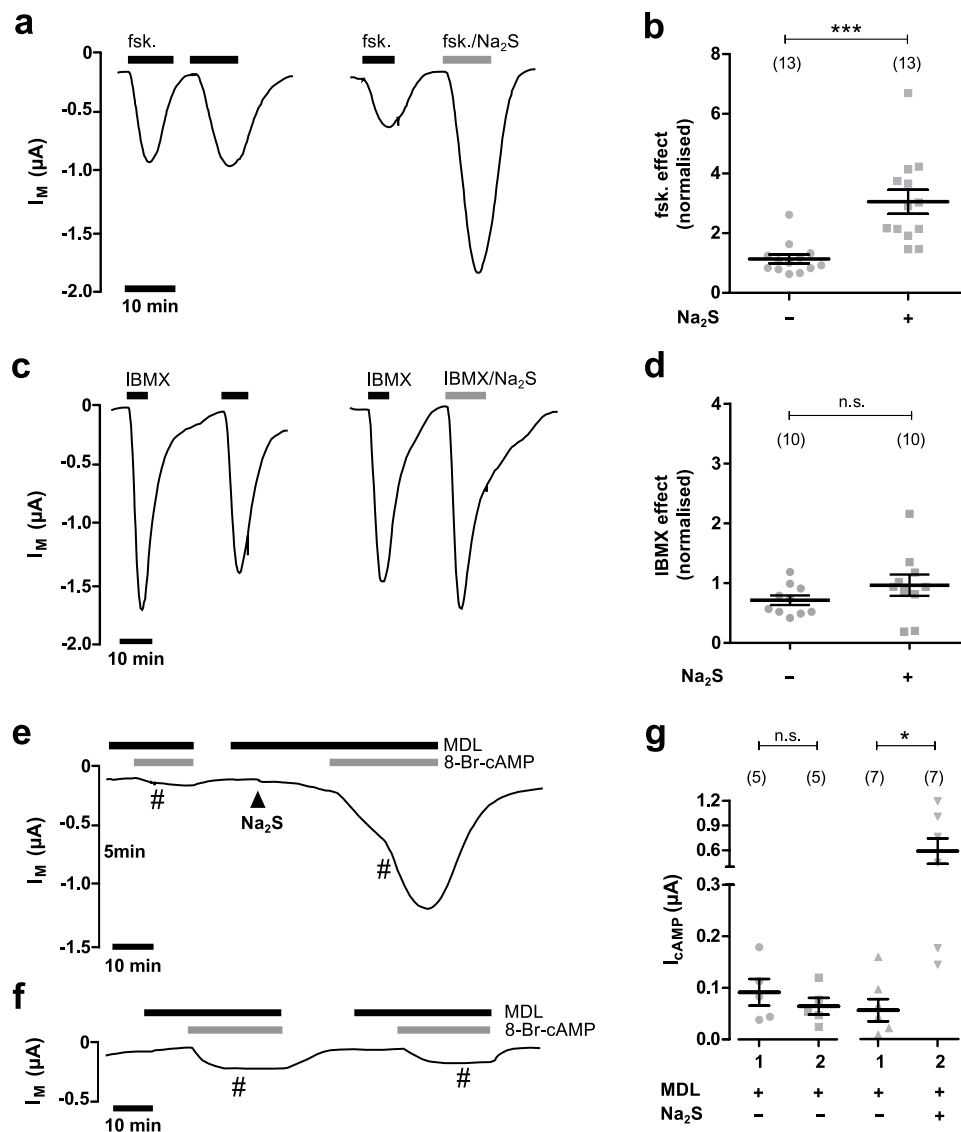


**Figure 4.** H<sub>2</sub>S targets phosphodiesterase rather than adenylyl cyclase. **(a)** Representative current traces of TEVC recordings of CFTR-expressing oocytes. Transmembrane currents ( $I_M$ ) were recorded and oocytes were either exposed twice to forskolin (fsk, 5  $\mu$ M; black bars; left trace) or first to forskolin and then to a combination of forskolin and 50  $\mu$ M Na<sub>2</sub>S (grey bar; right trace). **(b)** Statistical analysis of data obtained from experiments as shown in panel a. Depicted are normalised values from individual experiments (grey symbols) as well as means  $\pm$  SEM of forskolin (fsk.) effects. This represents the ratio of the first and second current stimulated by forskolin (\*\**P*  $\leq$  0.001, Mann-Whitney test). **(c)** Representative current traces of TEVC recordings of CFTR-expressing oocytes. Oocytes were either exposed twice to IBMX (1 mM; black bars; left trace) or first to IBMX and then to a combination of IBMX and 50  $\mu$ M Na<sub>2</sub>S (grey bar; right trace). **(d)** Statistical analysis of data obtained from experiments as shown in panel c. Depicted are normalised values from individual experiments (grey symbols) as well as means  $\pm$  SEM of IBMX effects. This represents the ratio of the first and second current stimulated by IBMX Student's unpaired t-test with Welch's correction). **(e, f)** Representative current traces of TEVC recordings of CFTR-expressing oocytes. **(f)** Oocytes were exposed twice to membrane-permeable 8-Br-cAMP (100  $\mu$ M, grey bars) in the presence of the AC-inhibitor MDL 12330 A (MDL, 20  $\mu$ M; black bars). The perfusion was stopped (indicated by the number symbol) when 8-Br-cAMP was in the perfusion chambers in order to avoid massive consumption of this compound. Perfusion was started again at the time of drug removal. **(e)** The same protocol was employed, with the exception that Na<sub>2</sub>S (50  $\mu$ M, black arrowhead) was applied before the second exposure to 8-Br-cAMP. **(g)** Statistical analysis of data obtained from experiments as shown in panels e and f. Depicted are values of the first (1) and second (2) 8-Br-cAMP-induced current ( $I_{cAMP}$ ) from individual experiments (grey symbols) as well as means  $\pm$  SEM (\*\**P*  $\leq$  0.01, Student's paired t-test). Numbers of experiments (n) are indicated in parentheses.

smaller than the first one. This is consistent with previous reports<sup>23</sup> and can be explained by a desensitisation in response to compounds which lead to a strong increase in intracellular cAMP<sup>26</sup>. The lack of a pronounced effect of H<sub>2</sub>S after initial stimulation with forskolin/IBMX is likely explained by the fact that Na<sub>2</sub>S alone is a much weaker stimulator of CFTR activity than forskolin/IBMX (as shown in Fig. 1a) and its effect is lost within the desensitisation after exposure to these compounds. Nevertheless, we found that H<sub>2</sub>S potentiated the second effect of forskolin and IBMX, indicating that the effect of H<sub>2</sub>S is additive to that of forskolin/IBMX. Furthermore, the H<sub>2</sub>S-induced activation of CFTR was lost in the presence of the AC inhibitor MDL12330A as well as the PKA antagonist cAMPS-Rp. These data indicate that H<sub>2</sub>S activates CFTR via the cAMP/PKA signalling axis, a finding which is consistent with a previous study demonstrating an increase in intracellular cAMP concentrations by H<sub>2</sub>S in *Xenopus* oocytes<sup>27</sup>. H<sub>2</sub>S is membrane-permeable<sup>28</sup> and might target AC in order to stimulate cAMP production. It has been previously shown that H<sub>2</sub>S either stimulates<sup>27,29</sup> or inhibits<sup>30,31</sup> AC activity, indicating that this enzyme represents indeed a molecular target for H<sub>2</sub>S. However, we found that H<sub>2</sub>S was able to potentiate the stimulation of CFTR by the AC-activator forskolin, but not by a high concentration (1 mM) of the PDE inhibitor IBMX. If H<sub>2</sub>S was acting on AC, there should be an additional effect over that of PDE inhibition alone – irrespective of the concentration of the PDE inhibitor. These data therefore suggest that H<sub>2</sub>S targets degradation rather than production of cAMP. However, these experiments alone do not justify a definite conclusion on the target for H<sub>2</sub>S. Based on the experiment using forskolin alone, a potential effect of H<sub>2</sub>S on AC cannot be ruled out completely. Forskolin increases the affinity of two cytoplasmic domains (C1 and C2) of AC for each other and enhances its activity<sup>32</sup>. In the presence of forskolin, AC becomes more sensitive to e.g. G<sub>so</sub><sup>32</sup>, suggesting that it is possible that there is a synergistic activation of AC by H<sub>2</sub>S in the presence of forskolin, but not in the presence of IBMX.

In addition to inhibiting PDEs, IBMX inhibits adenosine receptors, including endogenous adenosine receptors in *Xenopus* oocytes. Activation of these receptors inhibits AC and antagonising the receptor with IBMX might therefore elevate cAMP-concentrations – irrespective of the block of PDE-mediated degradation of cAMP. However, as shown in a study by Kobayashi *et al.* the receptors need to be activated by a ligand (adenosine) in order to generate a current signal in oocytes and this does not occur with a perfusion system as employed in our study<sup>33</sup>. Furthermore, it is not possible to discriminate between cGMP- and cAMP-PDEs using IBMX. It is possible that cGMP activates CFTR in *Xenopus* oocytes<sup>34</sup>, however, if H<sub>2</sub>S acted via cGMP, the effects of Na<sub>2</sub>S should not be sensitive to the adenylyl cyclase inhibitor MDL. This is further confirmed by the fact that H<sub>2</sub>S potentiated the stimulation of CFTR by exogenous membrane-permeable 8-Br-cAMP under conditions where endogenous cAMP production was blocked by the AC inhibitor MDL 12330A. The increased CFTR stimulation by 8-Br-cAMP in the presence of H<sub>2</sub>S can only be explained by impaired degradation of 8-Br-cAMP by endogenous PDE activity. Consistent with this hypothesis, several studies demonstrated that H<sub>2</sub>S is able to inhibit cAMP and cGMP degradation by PDEs<sup>35–37</sup>.

Most interestingly, small amounts (nano- to lower micro-molar range) of the sulphur salt NaHS inhibited PDE-mediated cAMP breakdown in cell-free systems<sup>35,37</sup>, suggesting that H<sub>2</sub>S might directly interfere with PDE activity – independently of cellular signalling cascades. This might be the result of an interference of H<sub>2</sub>S with zinc, thereby reducing the activity of zinc-dependent PDE<sup>35</sup>. Alternatively, H<sub>2</sub>S might target cysteine residues in the enzyme by persulfidation<sup>35</sup>. However, H<sub>2</sub>S alone cannot modify thiol groups<sup>38</sup>, whereas derivatives of H<sub>2</sub>S such as polysulfides<sup>13</sup> or nitroxyl, which might be formed in the cytoplasm of cells, are able to do so<sup>38</sup>. The precise mechanisms how H<sub>2</sub>S regulates PDE function remain to be elucidated; however, the *Xenopus* oocyte might be a useful model in order to address these questions.

In sum, we provide evidence that H<sub>2</sub>S inhibits endogenous PDE in the *Xenopus* oocyte, which likely results in an accumulation of cAMP and downstream activation of CFTR via PKA. This scenario, however, requires a constitutive production of cAMP in these cells. *Xenopus* oocytes are arrested in the G2 stage of meiosis I<sup>39</sup>. The G2 arrest is maintained by AC-mediated production of cAMP which is believed to prevent oocyte maturation via PKA-mediated signalling events<sup>39–41</sup>. Hence, there is a constitutive production of cAMP in *Xenopus* oocytes. Furthermore, there is an endogenous PDE activity in these cells<sup>42</sup> and the activities of both AC as well as PDE determine the concentration of cAMP. When *Xenopus* oocytes are exposed to progesterone, cAMP levels decrease, the cells undergo nuclear membrane breakdown (GVBD) and mature into a fertilisable egg<sup>39</sup>. This process is inhibited by IBMX<sup>42</sup>, again demonstrating that inhibition of PDE activity leads to an increase in the concentration of cAMP. Consistently, IBMX as well as H<sub>2</sub>S alone were able to stimulate CFTR activity in these cells in the present study.

Our data are consistent with an emerging body of evidence that H<sub>2</sub>S targets the cAMP-signalling axis. Whereas this study and others<sup>27,29</sup> provide evidence for an activation of the cAMP-pathway by H<sub>2</sub>S, inhibition of cAMP-signalling has also been reported<sup>43–45</sup>. A study by Lu *et al.* demonstrated inhibition of AC and stimulation of PDE by NaHS in AS4.1 cells<sup>44</sup>. These inconsistent findings suggest that the net-effect of H<sub>2</sub>S on cAMP signalling depends not only on whether AC or PDE is targeted by H<sub>2</sub>S, but also on the precise molecular repertoire of the cAMP-regulating machinery. In humans, ten isoforms of AC have been identified and there are 11 members of the PDE protein family which can generate nearly 100 different subtypes<sup>46</sup>. The specific isoform expression in a cell might critically determine whether H<sub>2</sub>S activates or inhibits cAMP-signalling. This is especially important, since H<sub>2</sub>S will diffuse across cell membranes in an unspecific manner and hence specificity is likely not achieved by membrane receptors but possibly by the subtype repertoire of intracellular signalling molecules.

In epithelia, H<sub>2</sub>S exerts pro-secretory or anti-absorptive effects<sup>15,47</sup> and we recently suggested a concept by which epithelia use their electrolyte and liquid transport machinery as a defence mechanism in order to flush potential sources for harmful amounts of H<sub>2</sub>S from the epithelial surfaces<sup>15</sup>. The herein reported cAMP-mediated stimulation of CFTR activity would be consistent with a pro-secretory action on chloride-secreting epithelia. A recent study demonstrated a CFTR-mediated chloride secretion across rat vaginal epithelial preparations<sup>21</sup>. The authors speculated that this might be due to an increase in cAMP<sup>21</sup> and our findings would support this hypothesis. Since H<sub>2</sub>S is not directly targeting CFTR, the PDE repertoire of epithelial cells will determine whether or not H<sub>2</sub>S triggers CFTR-mediated electrolyte secretion.



Aside from the pro-secretory effects, H<sub>2</sub>S prevents liquid absorption by sodium-transporting epithelia<sup>48–50</sup>. In these epithelia, cAMP/PKA signalling stimulates sodium absorption by an increase in the membrane abundance of sodium transporting molecules such as the epithelial sodium channel (ENaC)<sup>51,52</sup>. Interestingly, we recently showed that H<sub>2</sub>S prevents this cAMP-mediated increase in ENaC abundance in sodium-absorbing lung epithelial cells by yet unidentified mechanisms<sup>50</sup>. Furthermore, H<sub>2</sub>S did not enhance cAMP-mediated chloride secretion in primarily sodium absorbing pig airway surface epithelia (data not shown). Nevertheless, this illustrates that – depending on the specific enzymatic repertoire of the cAMP signalling axis – H<sub>2</sub>S might trigger cAMP-mediated electrolyte secretion in a fraction of epithelial cells, whilst simultaneously preventing enhanced electrolyte absorption in other cells. The herein reported data thus provide a step further in understanding the mechanisms of how H<sub>2</sub>S elicits a switch from absorptive to secretory electrolyte and water transport in epithelia.

## Methods

**Isolation of *Xenopus laevis* oocytes.** All animal experiments were performed in accordance with the German animal welfare law and had been declared to the Animal Welfare Officer of the University (Registration No.: M\_ 478 and M\_ 549). The animal housing facility was licensed by the local authorities (Az: FD 62 - §11 JLU Tierphysiologie). The methods used to euthanize the animals humanely were consistent with the recommendations of the AVMA Guidelines for the Euthanasia of Animals. All procedures and experimental protocols were approved by the Animal Welfare Officer of the University as well as the regional council of Giessen (Registration No.: M\_ 478 and M\_ 549).

Oocytes of stages V/VI were isolated from freshly dissected *Xenopus laevis* ovaries and defolliculated exactly as previously described<sup>53</sup>. Isolated oocytes were stored at 16 °C in an oocyte culture solution containing 90 mM NaCl, 1 mM KCl, 2 mM CaCl<sub>2</sub>, 5 mM 4-(2-hydroxyethyl)-1-piperazineethanesulfonic acid (HEPES), 2.5 mM sodium pyruvate, 0.06 mM penicillin G and 0.02 mM streptomycin sulfate at pH 7.4.

**CFTR-cRNA synthesis and injection into oocytes.** The plasmid construct for human CFTR (in pGEM-HE) was a kind gift from Professor Blanche Schwappach (University of Göttingen, Germany). Plasmids were linearised with MluI (Promega, Mannheim, Germany) and subsequently *in vitro* transcribed with the RiboMAX Large Scale RNA Production System (Promega) using T7 RNA polymerase. CFTR-cRNA was diluted with diethyl pyrocarbonate (DEPC)-treated water to a final concentration of 250 ng/μl. Fifty-one nanoliters of CFTR-cRNA were injected into oocytes with a Nanoliter-Injector (Drummond Scientific, Broomall, Pennsylvania, USA) yielding final concentrations of 12.5 ng RNA/oocyte. Injected oocytes were cultured for 2–5 days at 16 °C in the oocyte culture solution.

**Microelectrode recordings (Two-Electrode Voltage-Clamp, TEVC).** CFTR-expressing oocytes were placed in a Lucite chamber which was continuously perfused with oocyte ringer solution (ORS) containing 90 mM NaCl, 1 mM KCl, 2 mM CaCl<sub>2</sub>, 5 mM HEPES at pH 7.4. Chlorinated silver wires served as recording electrodes and were mounted into borosilicate glass capillaries (Hilgenberg, Malsfeld, Germany) with an outer diameter of 1.2 mm, which were pulled to microelectrodes with a DMZ universal puller (Zeitz-Instruments, Martinsried, Germany) and filled with 1 M KCl. Ag/AgCl wires were used as reference electrodes and placed directly into the recording chamber. The membrane voltage was clamped to –60 mV using a TEVC amplifier (Warner Instruments, Hamden, Connecticut, USA). Transmembrane currents (I<sub>M</sub>) were low-pass filtered at 1000 Hertz (Frequency Devices 902, Haverhill, Massachusetts, USA) and continuously recorded with a strip chart recorder (Kipp&Zonen, Delft, The Netherlands).

**Determination of evaporative loss of H<sub>2</sub>S from buffer solutions.** The equilibration of H<sub>2</sub>S with its concentration in air will eventually lead to evaporative loss of this gas from the experimental buffer solutions<sup>54</sup>. Therefore the relative concentration of H<sub>2</sub>S in ORS was determined at various time points after administration of 50 μM Na<sub>2</sub>S by the formation of methylene blue. Samples (300 μl) of the solutions were mixed with 500 μl of 4% zinc acetate and incubated on ice for at least 30 min. Afterwards, 200 μl of 0.1% dimethylphenylendiamine sulfate (in 5 M HCl) and 100 μl of 50 mM FeCl<sub>3</sub> were added. Samples were vortexed, centrifuged at 5000 × g and incubated for 5 min at room temperature. The absorption of methylene blue was measured at 670 nm with a Vis-spectrophotometer (Kruess Optronic, Hamburg, Germany).

**Chemicals and solutions.** In order to apply H<sub>2</sub>S, the sulfur salt Na<sub>2</sub>S (Sigma, Taufkirchen, Germany) or the slow releasing H<sub>2</sub>S donor GYY4137 (Santa Cruz, Biotechnology, Dallas, Texas, USA) were employed. Na<sub>2</sub>S was prepared as a stock solution of 50 mM in ORS freshly before experiments and immediately diluted to final working concentrations in order to prevent evaporative loss of H<sub>2</sub>S from the experimental solutions. Stock solutions of 100 mM GYY4137 were prepared in H<sub>2</sub>O and stored at –20 °C. Forskolin (MoBiTec, Göttingen, Germany) was used as a stimulator of adenylyl cyclase and stock solutions of 10 mM were prepared in dimethyl sulfoxide (DMSO, Sigma) and stored at –20 °C. The phosphodiesterase inhibitor 3-isobutyl-1-methylxanthine (IBMX; Sigma, Taufkirchen, Germany) was dissolved to 100 mM in DMSO and stored at +4 °C. The adenylyl cyclase inhibitor MDL 12330 A hydrochloride (MDL; Tocris Bioscience, Bristol, UK) was dissolved to 20 mM in DMSO and stored at +4 °C. cAMPS-Rp (Tocris Bioscience) was used as a competitive antagonist of cAMP-induced Protein Kinase A (PKA). Stock solutions of cAMPS-Rp were prepared to 10 mM in H<sub>2</sub>O and stored at –20 °C. cAMPS-Rp was injected into *Xenopus* oocytes during TEVC experiments. Therefore, stock solutions of cAMPS-Rp were diluted 1:1 with an intracellular-analogous solution (IAS) which contained 20 mM NaCl, 130 mM KCl, 2 mM MgCl<sub>2</sub> and 5 mM HEPES at pH 7.3. This mixture (9.2 nl) was injected into oocytes, leading to concentrations of ~87 μM cAMPS-Rp per oocyte. Corresponding control experiments were performed with IAS. The membrane permeable cAMP-analogue 8-Br-cAMP (Tocris Bioscience) was prepared as a 10 mM stock solution in H<sub>2</sub>O and stored at –20 °C.

**Drug application.** Drugs were generally applied using a gravity-driven perfusion system. In order to reduce the amount of drugs needed, the membrane-permeable cAMP-analogue 8-Br-cAMP was washed into the perfusion chamber and the perfusion was stopped afterwards. The PKA inhibitor cAMPS-Rp was directly injected into the oocytes since this strategy was established earlier and achieved adequate inhibition of PKA<sup>55</sup>.

**Statistical analysis.** For electrophysiological transmembrane recordings, outward-anion currents are defined as negative current signals and depicted in all figures as downward-deflections of the current traces. Data are presented as individual data points (grey symbols) as well as means  $\pm$  standard error of the mean (SEM). The number of individual oocytes is indicated with 'n', whereas the number of donor frogs is represented by 'N'. Statistical analysis of data was performed with GraphPad Prism version 5 (La Jolla, California, USA). Data were analysed for normal distribution by the Kolmogorov-Smirnov test. For paired experiments, Student's paired *t*-test or non-parametric Wilcoxon matched-pairs test (two-tailed) were used. Independent experiments were compared with Student's unpaired *t*-test or non-parametric Mann-Whitney test (two-tailed). Multiple comparison analysis was performed by Kruskal-Wallis test followed by Dunn's Multiple Comparison Test. *P*-values  $\leq 0.05$  were regarded as statistically significant and marked with an asterisk (\*). *P*-values  $\leq 0.01$  and  $\leq 0.001$  were marked with "\*\*\*" and "\*\*\*\*", respectively.

## References

- Ratjen, F. *et al.* Cystic fibrosis. *Nature reviews. Disease primers* **1**, 15010, doi:10.1038/nrdp.2015.10 (2015).
- Farinha, C. M., Swiatecka-Urban, A., Brautigan, D. L. & Jordan, P. Regulatory Crosstalk by Protein Kinases on CFTR Trafficking and Activity. *Frontiers in chemistry* **4**, 1, doi:10.3389/fchem.2016.00001 (2016).
- Berger, A. L., Ikuma, M. & Welsh, M. J. Normal gating of CFTR requires ATP binding to both nucleotide-binding domains and hydrolysis at the second nucleotide-binding domain. *Proceedings of the National Academy of Sciences of the United States of America* **102**, 455–460, doi:10.1073/pnas.0408575102 (2005).
- Sheppard, D. N. & Welsh, M. J. Structure and function of the CFTR chloride channel. *Physiological Reviews* **79**, S23–45 (1999).
- Boucher, R. C. New concepts of the pathogenesis of cystic fibrosis lung disease. *The European respiratory journal: official journal of the European Society for Clinical Respiratory Physiology* **23**, 146–158 (2004).
- Widdicombe, J. H. & Wine, J. J. Airway Gland Structure and Function. *Physiological Reviews* **95**, 1241–1319, doi:10.1152/physrev.00039.2014 (2015).
- Shamsuddin, A. K. M. & Quinton, P. M. Surface Fluid Absorption and Secretion in Small Airways. *The Journal of physiology*, doi:10.1113/jphysiol.2012.230714 (2012).
- Kunzelmann, K. & Mehta, A. CFTR: a hub for kinases and crosstalk of cAMP and Ca<sup>2+</sup>. *The FEBS journal* **280**, 4417–4429, doi:10.1111/febs.12457 (2013).
- Wang, R. Physiological implications of hydrogen sulfide: a whiff exploration that blossomed. *Physiological reviews* **92**, 791–896, doi:10.1152/physrev.00017.2011 (2012).
- Wallace, J. L. & Wang, R. Hydrogen sulfide-based therapeutics: exploiting a unique but ubiquitous gasotransmitter. *Nature Reviews Drug Discovery* **14**, 329–345, doi:10.1038/nrd4433 (2015).
- Kimura, H. Metabolic turnover of hydrogen sulfide. *Frontiers in physiology* **3**, 101, doi:10.3389/fphys.2012.00101 (2012).
- Bailey, T. S., Zakharov, L. N. & Pluth, M. D. Understanding Hydrogen Sulfide Storage: Probing Conditions for Sulfide Release from Hydrodisulfides. *Journal of the American Chemical Society* **136**, 10573–10576, doi:10.1021/ja505371z (2014).
- Kimura, H. Hydrogen sulfide and polysulfides as biological mediators. *Molecules (Basel, Switzerland)* **19**, 16146–16157, doi:10.3390/molecules191016146 (2014).
- Olson, K. R. Hydrogen sulfide as an oxygen sensor. *Clinical chemistry and laboratory medicine: CCLM / FESCC* **51**, 623–632, doi:10.1515/cclm-2012-0551 (2013).
- Pouokam, E. & Althaus, M. Epithelial Electrolyte Transport Physiology and the Gasotransmitter Hydrogen Sulfide. *Oxidative Medicine and Cellular Longevity* **2016**, 4723416, doi:10.1155/2016/4723416 (2016).
- Macfarlane, G. T., Gibson, G. R. & Cummings, J. H. Comparison of fermentation reactions in different regions of the human colon. *Journal of Applied Bacteriology* **72**, 57–64, doi:10.1111/j.1365-2672.1992.tb04882.x (1992).
- Blachier, F. *et al.* Luminal sulfide and large intestine mucosa: friend or foe? *Amino Acids* **39**, 335–347, doi:10.1007/s00726-009-0445-2 (2010).
- Hennig, B. & Diener, M. Actions of hydrogen sulphide on ion transport across rat distal colon. *British journal of pharmacology* **158**, 1263–1275, doi:10.1111/j.1476-5381.2009.00385.x (2009).
- Pouokam, E. & Diener, M. Mechanisms of actions of hydrogen sulphide on rat distal colonic epithelium. *British journal of pharmacology* **162**, 392–404, doi:10.1111/j.1476-5381.2010.01026.x (2011).
- Schicho, R. *et al.* Hydrogen sulfide is a novel prosecretory neuromodulator in the Guinea-pig and human colon. *Gastroenterology* **131**, 1542–1552, doi:10.1053/j.gastro.2006.08.035 (2006).
- Sun, Q. *et al.* Hydrogen Sulfide Facilitates Vaginal Lubrication by Activation of Epithelial ATP-Sensitive K(+) Channels and Cystic Fibrosis Transmembrane Conductance Regulator. *The journal of sexual medicine* **13**, 798–807, doi:10.1016/j.jsxm.2016.03.001 (2016).
- Lee, Z. W. *et al.* The slow-releasing hydrogen sulfide donor, GYY4137, exhibits novel anti-cancer effects *in vitro* and *in vivo*. *PLoS ONE* **6**, e21077, doi:10.1371/journal.pone.0021077 (2011).
- Vitzthum, C., Clauss, W. G. & Fronius, M. Mechanosensitive activation of CFTR by increased cell volume and hydrostatic pressure but not shear stress. *Biochimica et biophysica acta* **1848**, 2942–2951, doi:10.1016/j.bbame.2015.09.009 (2015).
- Ostedgaard, L. S. *et al.* The DeltaF508 mutation causes CFTR misprocessing and cystic fibrosis-like disease in pigs. *Science translational medicine* **3**, 74ra24, doi:10.1126/scitranslmed.3001868 (2011).
- Kimura, Y., Dargusch, R., Schubert, D. & Kimura, H. Hydrogen sulfide protects HT22 neuronal cells from oxidative stress. *Antioxid Redox Signal* **8**, 661–670, doi:10.1089/ars.2006.8.661 (2006).
- Moran, O. & Zegarra-Moran, O. On the measurement of the functional properties of the CFTR. *Journal of cystic fibrosis: official journal of the European Cystic Fibrosis Society* **7**, 483–494, doi:10.1016/j.jcf.2008.05.003 (2008).
- Kimura, H. Hydrogen sulfide induces cyclic AMP and modulates the NMDA receptor. *Biochemical and biophysical research communications* **267**, 129–133, doi:10.1006/bbrc.1999.1915 (2000).
- Mathai, J. C. *et al.* No facilitator required for membrane transport of hydrogen sulfide. *Proceedings of the National Academy of Sciences of the United States of America* **106**, 16633–16638, doi:10.1073/pnas.0902952106 (2009).
- Muzaffar, S. *et al.* H<sub>2</sub>S-donating sildenafil (ACS6) inhibits superoxide formation and gp91phox expression in arterial endothelial cells: role of protein kinases A and G. *British journal of pharmacology* **155**, 984–994, doi:10.1038/bjp.2008.326 (2008).
- Nagpure, B. V. & Bian, J.-S. Hydrogen Sulfide Inhibits A2A Adenosine Receptor Agonist Induced  $\beta$ -Amyloid Production in SH-SY5Y Neuroblastoma Cells via a cAMP Dependent Pathway. *PloS one* **9**, e88508, doi:10.1371/journal.pone.0088508 (2014).
- Yang, H.-Y., Wu, Z.-Y., Wood, M., Whiteman, M. & Bian, J.-S. Hydrogen sulfide attenuates opioid dependence by suppression of adenylyl cyclase/cAMP pathway. *Antioxidants & redox signaling* **20**, 31–41, doi:10.1089/ars.2012.5119 (2014).

32. Yan, S. Z., Hahn, D., Huang, Z. H. & Tang, W. J. Two cytoplasmic domains of mammalian adenylyl cyclase form a Gs alpha- and forskolin-activated enzyme *in vitro*. *J Biol Chem* **271**, 10941–10945 (1996).
33. Kobayashi, T., Ikeda, K. & Kumanishi, T. Functional characterization of an endogenous *Xenopus* oocyte adenosine receptor. *Br J Pharmacol* **135**, 313–322, doi:10.1038/sj.bjp.0704475 (2002).
34. Sullivan, S. K., Agellon, L. B. & Schick, R. Identification and partial characterization of a domain in CFTR that may bind cyclic nucleotides directly. *Curr Biol* **5**, 1159–1167 (1995).
35. Bucci, M. *et al.* Hydrogen sulfide is an endogenous inhibitor of phosphodiesterase activity. *Arteriosclerosis, thrombosis, and vascular biology* **30**, 1998–2004, doi:10.1161/ATVBAHA.110.209783 (2010).
36. Coletta, C. *et al.* Hydrogen sulfide and nitric oxide are mutually dependent in the regulation of angiogenesis and endothelium-dependent vasorelaxation. *Proceedings of the National Academy of Sciences of the United States of America* **109**, 9161–9166, doi:10.1073/pnas.1202916109 (2012).
37. Modis, K., Panopoulos, P., Coletta, C., Papapetropoulos, A. & Szabo, C. Hydrogen sulfide-mediated stimulation of mitochondrial electron transport involves inhibition of the mitochondrial phosphodiesterase 2A, elevation of cAMP and activation of protein kinase A. *Biochemical Pharmacology* **86**, 1311–1319, doi:10.1016/j.bcp.2013.08.064 (2013).
38. Filipovic, M. R. Vol. 230 29–59.
39. Duckworth, B. C., Weaver, J. S. & Ruderman, J. V. G2 arrest in *Xenopus* oocytes depends on phosphorylation of cdc25 by protein kinase A. *Proceedings of the National Academy of Sciences of the United States of America* **99**, 16794–16799, doi:10.1073/pnas.222661299 (2002).
40. Voronina, E. & Wessel, G. M. The regulation of oocyte maturation. *Current topics in developmental biology* **58**, 53–110 (2003).
41. Nader, N., Courjaret, R., Dib, M., Kulkarni, R. P. & Machaca, K. Release from *Xenopus* oocyte prophase I meiotic arrest is independent of a decrease in cAMP levels or PKA activity. *Development* **143**, 1926–1936, doi:10.1242/dev.136168 (2016).
42. Sadler, S. E. & Maller, J. L. *In vivo* regulation of cyclic AMP phosphodiesterase in *Xenopus* oocytes. Stimulation by insulin and insulin-like growth factor 1. *The Journal of biological chemistry* **262**, 10644–10650 (1987).
43. Yong, Q. C., Pan, T. T., Hu, L. F. & Bian, J. S. Negative regulation of beta-adrenergic function by hydrogen sulphide in the rat hearts. *J Mol Cell Cardiol* **44**, 701–710, doi:10.1016/j.yjmcc.2008.01.007 (2008).
44. Lu, M., Liu, Y. H., Ho, C. Y., Tiong, C. X. & Bian, J. S. Hydrogen sulfide regulates cAMP homeostasis and renin degranulation in As4.1 and rat renin-rich kidney cells. *Am J Physiol Cell Physiol* **302**, C59–66, doi:10.1152/ajpcell.00341.2010 (2012).
45. Lim, J. J., Liu, Y. H., Khin, E. S. & Bian, J. S. Vasoconstrictive effect of hydrogen sulfide involves downregulation of cAMP in vascular smooth muscle cells. *Am J Physiol Cell Physiol* **295**, C1261–1270, doi:10.1152/ajpcell.00195.2008 (2008).
46. Kokkonen, K. & Kass, D. A. Nanodomain Regulation of Cardiac Cyclic Nucleotide Signaling by Phosphodiesterases. *Annu Rev Pharmacol Toxicol* **57**, 455–479, doi:10.1146/annurev-pharmtox-010716-104756 (2017).
47. Pouokam, E., Steidle, J. & Diener, M. Regulation of colonic ion transport by gasotransmitters. *Biological & pharmaceutical bulletin* **34**, 789–793 (2011).
48. Althaus, M., Urness, K., Clauss, W., Baines, D. & Fronius, M. The gasotransmitter hydrogen sulphide decreases Na<sup>(+)</sup> transport across pulmonary epithelial cells. *British journal of pharmacology* **166**, 1946–1963, doi:10.1111/j.1476-5381.2012.01909.x (2012).
49. Erb, A. & Althaus, M. Actions of hydrogen sulfide on sodium transport processes across native distal lung epithelia (*Xenopus laevis*). *PLoS one* **9**, e100971, doi:10.1371/journal.pone.0100971 (2014).
50. Agné, A. M. *et al.* Hydrogen sulfide decreases  $\beta$ -adrenergic agonist-stimulated lung liquid clearance by inhibiting ENaC-mediated transepithelial sodium absorption. *American Journal of Physiology - Regulatory, Integrative and Comparative Physiology* **308**, R636–R649, doi:10.1152/ajpregu.00489.2014 (2015).
51. Walters, D. V., Ramsden, C. A. & Olver, R. E. Dibutyl cAMP induces a gestation-dependent absorption of fetal lung liquid. *Journal of applied physiology (Bethesda, Md. : 1985)* **68**, 2054–2059 (1990).
52. Baines, D. Kinases as targets for ENaC regulation. *Current molecular pharmacology* **6**, 50–64 (2013).
53. Perniss, A., Wolf, A., Wichmann, L., Schonberger, M. & Althaus, M. Evans Blue is not a suitable inhibitor of the epithelial sodium channel delta-subunit. *Biochemical and biophysical research communications* **466**, 468–474, doi:10.1016/j.bbrc.2015.09.052 (2015).
54. DeLeon, E. R., Stoy, G. F. & Olson, K. R. Passive loss of hydrogen sulfide in biological experiments. *Analytical biochemistry* **421**, 203–207, doi:10.1016/j.ab.2011.10.016 (2012).
55. Weber, W. M., Cuppens, H., Cassiman, J. J., Clauss, W. & Van Driessche, W. Capacitance measurements reveal different pathways for the activation of CFTR. *Pflugers Arch* **438**, 561–569 (1999).

## Acknowledgements

The authors thank Liesa Kristin Beuter as well as Raphael J. Courjaret and Khaled Machaca (Weill Cornell Medicine Qatar) for help with some experiments and Mirjam Buß and Anja Schnecko for excellent technical assistance. Nikolaus P. Dittrich, Lukas Wichmann and Pawel P. Szczesniak are acknowledged for helpful comments on the manuscript. This work is supported by a grant from the German Research Foundation (DFG; AL1453/1-2) to MA.

## Author Contributions

M.A. designed experiments, A.P., K.P. and M.N. performed experiments. All authors analysed and interpreted data. M.A. wrote the manuscript and prepared figures. All authors reviewed the manuscript.

## Additional Information

**Competing Interests:** The authors declare that they have no competing interests.

**Publisher's note:** Springer Nature remains neutral with regard to jurisdictional claims in published maps and institutional affiliations.



**Open Access** This article is licensed under a Creative Commons Attribution 4.0 International License, which permits use, sharing, adaptation, distribution and reproduction in any medium or format, as long as you give appropriate credit to the original author(s) and the source, provide a link to the Creative Commons license, and indicate if changes were made. The images or other third party material in this article are included in the article's Creative Commons license, unless indicated otherwise in a credit line to the material. If material is not included in the article's Creative Commons license and your intended use is not permitted by statutory regulation or exceeds the permitted use, you will need to obtain permission directly from the copyright holder. To view a copy of this license, visit <http://creativecommons.org/licenses/by/4.0/>.

© The Author(s) 2017